

CORRIGENDA

V. S. BELIKOV and Ya. I. KOLESNICHENKO, "Edge-Localized Thermonuclear Magnetoacoustic-Cyclotron Instability in Tokamaks," *Fusion Technol.*, **25**, 258 (1994).

On p. 263, the first sentence of column 2 should read as follows: We see that the relative alpha-particle density in the experiment is $n_\alpha/n \sim 10^{-4}$, which well exceeds the threshold values of n_α^{cr}/n_i for $l > 3$ given by Table III.

Table III contains erroneous data. The following table is correct.

TABLE III
 n_α^{cr}/n_D for $T_D = 2$ keV

l	$\nu + \tau_s/\tau_n$			
	3	4	5	6
3	9.0×10^{-4}	4.7×10^{-4}	3.1×10^{-4}	2.6×10^{-4}
4	1.5×10^{-5}	7.1×10^{-6}	4.3×10^{-6}	3.5×10^{-6}

A. M. MESSIAEN, "Experimental Transport Analysis and Scaling to Reactors," *Trans. Fusion Technol.*, **25**, 2T, 127 (1994).

The original figures for this paper were inadvertently omitted. They appear on the following pages.

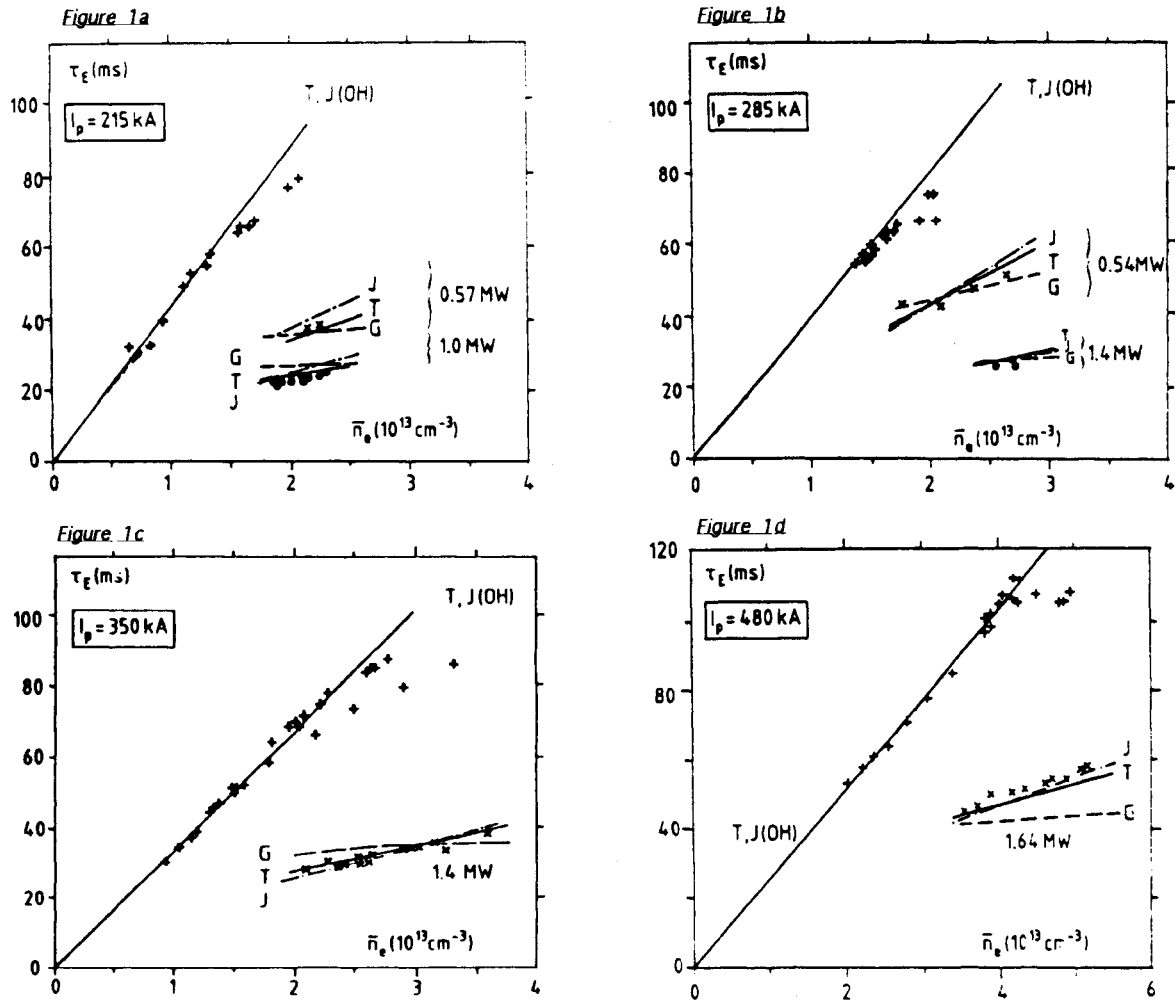


Fig.1: Evolution of τ_E versus the central average chord density for ohmic discharges (OH) and auxiliary heated discharges (with ICRH) for different plasma current. The predictions of neoalcalator scaling (for OH) and different scalings are added. (T: Equ.17, J: Equ.18, G:Equ.16).

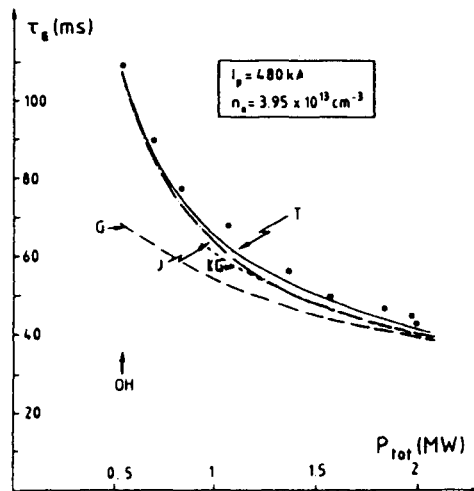


Fig.2: Power scan of the global energy confinement time τ_E versus the total power coupled to the plasma P_{TOT} (TEXTOR, case of ICRH additional heating : $P_{TOT} = P_{OH} + P_{RF}$). The predictions of different scaling laws are added. (T: Equ.17, J: Equ.18, G: Equ.16, K-G: Kaye-Goldston scaling; see Table 1).

Figure 3a

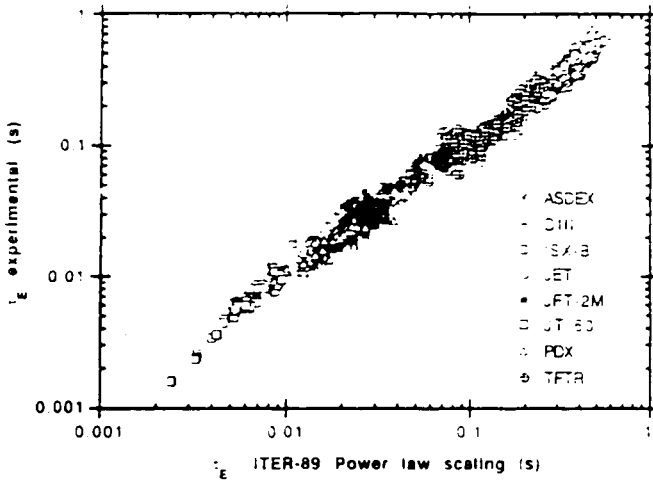


Figure 3b

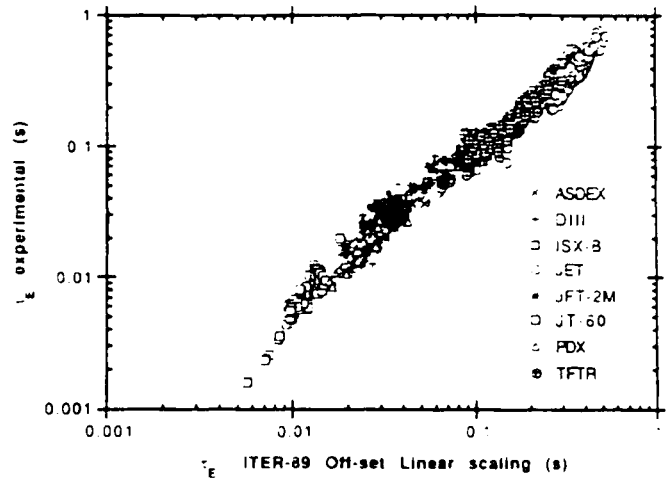


Fig.3: Comparison of the scalings with experimental data from different tokamaks
 (a) Experimental τ_E versus τ_E from the ITER-89 power law scaling;
 (b) Experimental τ_E versus τ_E from the ITER-89 offset-linear scaling.

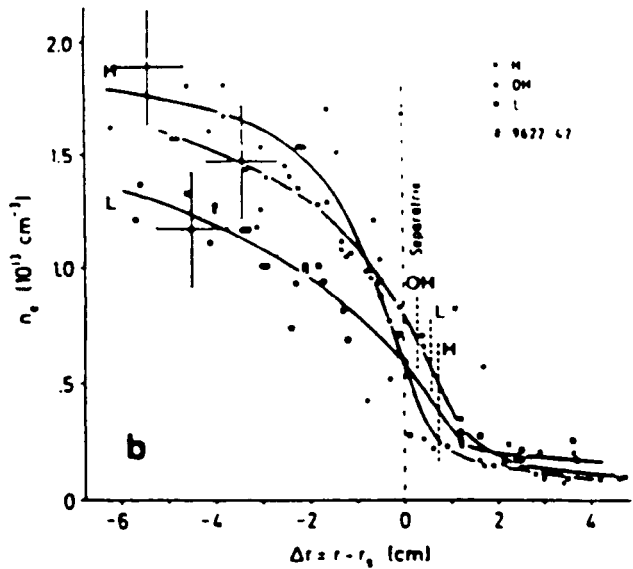
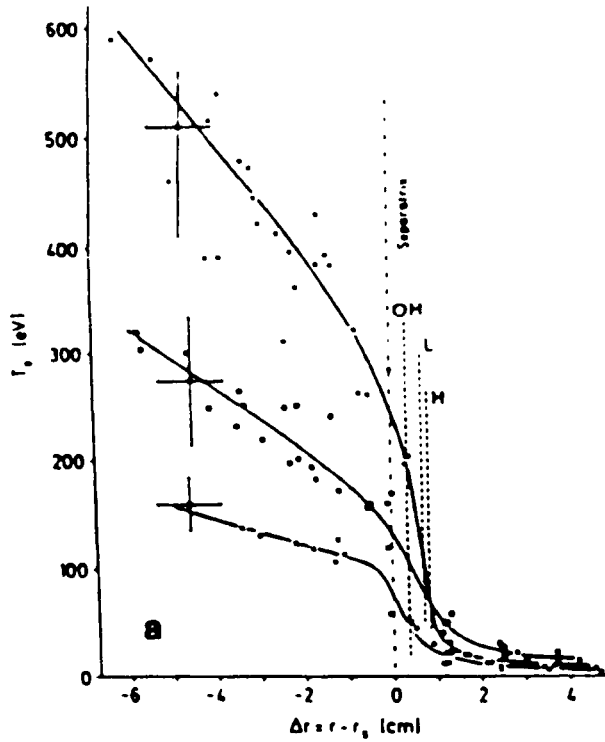


Fig.4: Radial profiles of (a) T_e and (b) n_e in the midplane over the separatrix vicinity for ohmically and NI-heated discharges in ASDEX [8]: $r=r_s$ is the nominal separatrix position according to magnetic signals. Vertical bars indicate separatrix positions determined from electron pressure profiles in the divertor chamber using the assumption $n_e T_e = \text{const.}$ along field lines.

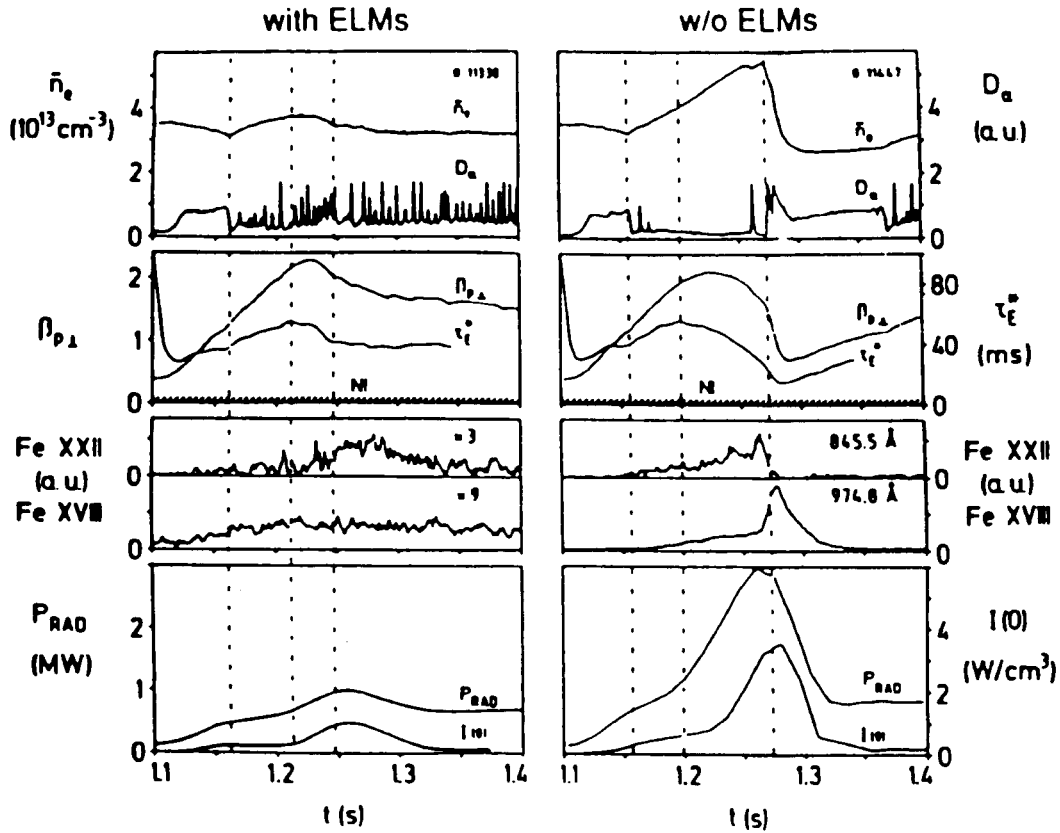


Fig. 5: Time evolution of various plasma parameters of H-mode discharges in ASDEX [8] with and without ELMs ($I_p = 0.32$ MA, $B_T = 2.17$ T, $P_{NI} = 3.3$ MW, $H^0 \rightarrow D^*$): line-averaged plasma density \bar{n}_e , D_α -light intensity in the divertor chamber, beta poloidal β_p , global energy confinement time τ_E^* ; Fe XVIII and Fe XXII line intensities (representative of ion radiation from $r/a = 2/3$ and the plasma centre), and finally the total and central radiation losses P_{RAD} and $I(0)$.

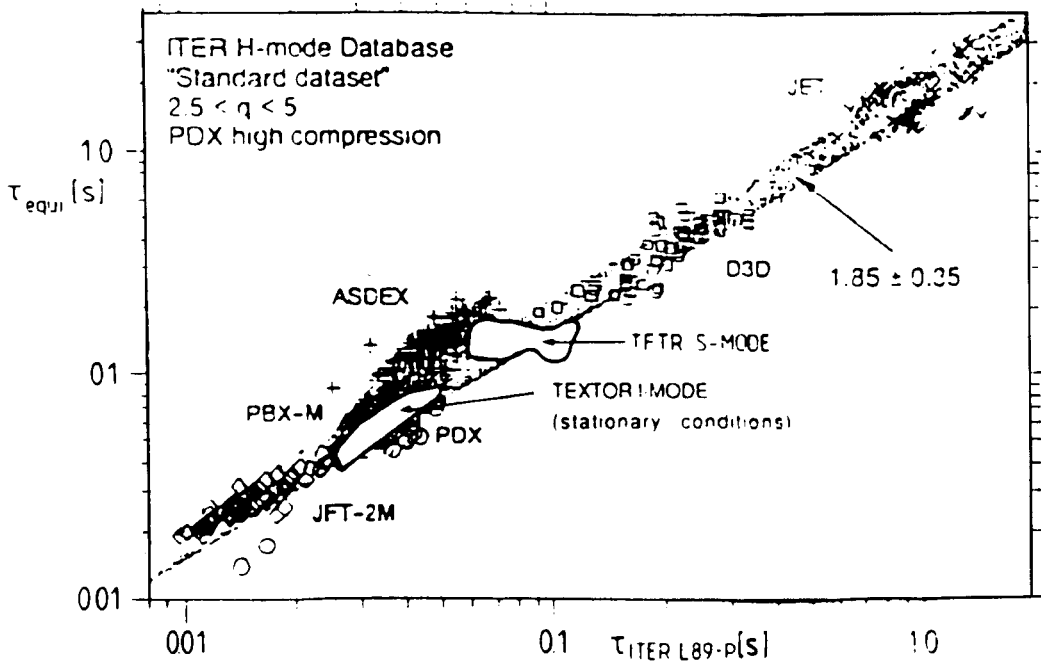


Fig. 6: Experimental confinement times compared with the ITER-L89-P scaling for L-mode for divertor machines operating in the H-mode, for the "supershots" of TFTR and for the I-mode of TEXTOR. The value of $f_H = 1.85$ is also indicated.